Memoria
de la Fundación La Salle de Ciencias Naturales
ISSN: 0037-8518 Versión impresa
ISSN: 2443-4698 Versión electrónica

Memoria de la Fundación La Salle de Ciencias Naturales, 2023, 81(191): 91-110

Article

Vertical Structure and trends in CO_2 at the CARIACO Ocean Time Series Station: 1995-2017

Yrene M. Astor, Laura Lorenzoni, Digna Rueda-Roa y Frank Muller-Karger

Abstract: Changes in the vertical structure of pH (total proton scale at 25 °C or pH_T), total alkalinity, total CO_2 (TCO_2), and partial pressure of CO_2 (pCO_2) were examined at the CARIACO Ocean Time Series station (10º30'N, 64º40'W) from December 1995 to January 2017. Long-term trends were studied in the three water masses present in the Cariaco Basin: the surface layer (SL, located between 0-100 m depth), the Subtropical Underwater (SUW, with minimum depths between the surface and 105 m and maximums between 30-165 m depending on the season) and the deep water (DW, with minimum depths between 175-380 m to the bottom). The seasonal detrended TCO_2 normalized to a constant salinity ($nTCO_2$) showed a positive trend 2.23 ± 0.43 µmol kg^{-1} yr^{-1} in the SL, associated with an increase in pCO_2 (3.06 ± 0.42 µatm yr^{-1}) and a decrease in pH (-0.0028 ± 0.0004 pH yr^{-1}). SUW and DW also exhibited increasing trends $nTCO_2$ (1.82 ± 0.42 and 4.46 ± 0.32 µmol kg^{-1} yr^{-1}, respectively). Between 2002 and 2017, an increase of 67 µmol kg^{-1} of TCO_2 was observed below 300 m at the CARIACO station. Overall, acidification trends were observed at the Cariaco station from the surface to the bottom, with an average of ~ -0.003 ± 0.0004 pH units per year. Air-sea CO_2 flux calculations showed an average net evasion of CO_2 from the sea to the air of 0.6 ± 2.2 mol C m^{-2} yr^{-1} for the period of observation.

Key words: Carbonate system; vertical and temporal variability; air-sea exchange; Cariaco Basin, Caribbean Sea; Venezuela

Estructura vertical y tendencias en el CO_2 en la estación Serie de Tiempo CARIACO: 1995-2017

Resumen: Se examinaron cambios en la estructura vertical del pH (escala total de protones a 25 °C o pH_T), la alcalinidad total, el CO_2 total (TCO_2) y la presión parcial de CO_2 (pCO_2) en la estación oceanográfica serie de tiempo CARIACO (10º30'N, 64º40'O) desde diciembre de 1995 hasta enero de 2017. Se estudiaron las tendencias a largo plazo en las tres masas de agua presentes en la cuenca de Cariaco: la capa superficial (SL, ubicada entre 0-100 m), la Subtropical (SUW, con profundidades mínimas entre la superficie y 105 m y máximas entre 30-165 m dependiendo de la temporada), y las aguas profundas (DW, con profundidades mínimas entre 175-380 m hasta el fondo). El TCO_2 desestacionalizado y normalizado a una salinidad constante ($nTCO_2$) mostró una tendencia positiva de 2,23 ± 0,43 µmol kg^{-1} $año^{-1}$ en la capa SL, relacionada con un aumento en pCO_2 (3.06 ± 0.42 µatm $año^{-1}$) y una disminución del pH (-0.0028 ± 0.0004 pH $año^{-1}$). SUW y DW también mostraron tendencias crecientes en $nTCO_2$ (1,82 ± 0,42 y 4,46 ± 0,32 µmol kg^{-1} $año^{-1}$, respectivamente). Entre 2002 y 2017, se observó un aumento de 67 µmol kg^{-1} de TCO_2 por debajo de 300 m en la estación CARIACO. En general, se observaron tendencias de acidificación en la estación Cariaco desde la superficie hasta el fondo, con un promedio de ~ -0.003 ± 0.0004 unidades de pH por año. Los cálculos del flujo de CO_2 entre el aire y el océano mostraron una evasión neta promedio de CO_2 desde el mar al aire de 0.6 ± 2.2 mol C m^{-2} $año^{-1}$ durante el período de observación.

Palabras clave: Sistema carbonatos; variabilidad vertical y temporal; intercambio aire mar; Fosa de Cariaco; Mar Caribe; Venezuela

Introduction

About 675 ± 80 PgC were released to the atmosphere by human activity between 1750 and 2018, increasing carbon dioxide (CO_2) in the atmosphere by more than 40% (Friedlingstein *et al.* 2019). Part of this carbon accumulates in the atmosphere, but a substantial amount is sequestered in carbon sinks such as the terrestrial biosphere or the ocean. The ocean has taken up about a third of the carbon emissions (Khatiwala *et al.* 2013), leading to a decrease in seawater pH and changes in the concentration of carbonate ions (CO_3^{2-}), and in the calcite (Ω_{cal}) and aragonite (Ω_{arag}) saturation states over time (Caldeira and Wickett 2003, Bates *et al.* 2012).

Long-term time series measurements are required to characterize changes in CO_2 in ocean waters and their relationship to other variables such as temperature, salinity, and the biology of any area (Santana-Casiano *et al.* 2007, Bates *et al.* 2012). Although long-term ocean time series observations are valuable platforms to evaluate the interannual variations and trends of surface seawater CO_2, few of them have described deep oceans trends of the carbonate system variables (González-Davila *et al.* 2010). The CARIACO Ocean Time Series program carried out relevant observations in the southern Caribbean Sea for over 21 years (November 1995 to January 2017). The geography and oceanographic setting of the Cariaco Basin have been described previously (Goñi *et al.* 2003, Muller-Karger *et al.* 2001, Muller-Karger *et al.* 2019). The seasonal variability of the carbonate system parameters for surface waters at the CARIACO station and their relationship to other properties have been addressed for different periods (Astor *et al.* 2005, Astor *et al.* 2013, Bates *et al.* 2014). Here we describe the changes in the vertical structure of carbonate system parameters at this location and re-examined the surface variability of CO_2 flux over the complete set of observations of this time series.

Methods

Field sampling

The CARIACO Ocean Time Series station was located on the eastern sub-basin of the Cariaco Basin off the coast of Venezuela (10º30'N, 64º40'W). Monthly observations were conducted from November 1995 to January 2017 using the R/V *Hermano Ginés* of the Margarita Marine Research Station (EDIMAR; Fundación La Salle de Ciencias Naturales, Venezuela). Samples for the carbonate system were collected at nearly monthly frequencies, with some interruptions over 21 years due to equipment malfunction. The most significant gaps occurred from May 2001 to March 2002, and June to August 2016.

Water samples for pH_T (total proton scale at 25 ºC) and total alkalinity (TA) were collected in 8-L Niskin bottles at 19 depths between 1 and 1310 m (bottom depth: 1380 m) using a CTD rosette system (SeaBird SBE 25). Measurements of pH_T were made on board within 1 h of sampling. TA samples were collected in 250-ml amber glass bottles and poisoned immediately with 50 µL of saturated mercuric chloride solution. Samples were stored at 4 ºC and analyzed within two months from sample collection. Further details about CARIACO sampling, preservation and storage have been covered extensively (Astor *et al.* 2005; 2013 and 2017).

Analytical procedures

Measurements of pH_T were made using the spectrophotometric technique developed by Clayton and Byrne (1993) and modified by DelValls and Dickson (1998) and Dickson *et al.* (2007). The pH_T method uses the dye meta-cresol purple (mCP) as the pH indicator. The determination of pH is based on the ratio of the wavelengths corresponding to the absorbance maxima of the base (578 nm, I^{2-}) and acid (434 nm, HI^{-}) ($R = {}_{578}A/{}_{434}A$). The unpurified forms of the dye absorb significantly at the wavelength of maximum absorption for the acid species (Liu *et al.* 2011). The presence of impurities in the indicator dye may cause uncertainty in the measured pH values that propagate into CO_2 equilibrium calculations of pCO_2, with errors ranging 11 to 200 µatm (Yao *et al.* 2007, DeGrandpre *et al.* 2014). The effects of impurities also vary from one indicator manufacturer to another, and from different batches of the same manufacturer (Yao *et al.* 2007), and they translate into lower calculated pH values, especially in surface waters where pH > 8.0 (Yao *et al.* 2007). Only one batch form of the mCP dye was used for the entire CARIACO set of observations, and it was in its unpurified form.

The ${}_{434}A_{imp}$ corrective model developed by Douglas and Byrne (2017) to correct pH measurements for mCP impurities was applied to the CARIACO data. The ${}_{434}A_{imp}$ correction yields improvements in pH accuracy on the order of 0.005 at low pH (~ 7.25) and 0.01 or more at higher pH (~ 8.25) (Douglas and Byrne, 2017). Using the corrected pH observations, new CO_2 equilibrium parameters and estimates of air-sea CO_2 flux were derived. The corrected CARIACO pH values were usually significantly lower than the uncorrected ones (paired t-student = 150, $p < 0.001$, $n = 3829$). For example, there was an average difference of -0.01 ± 0.004 for waters with a pH > 8.1 (typical surface waters). Waters with a pH < 7.6 (typical of deep waters) showed a smaller difference (-0.007 ± 0.002). Precision of pH measurements was around ± 0.003 pH units. All the results are reported at 25 ºC to avoid the effects of temperature on the analysis. Between December 1995 and May 2001, we used an Ocean Optics S1000 dual channel fiber optic spectrometer. This instrument was later replaced with an Ocean Optics S2000 in March 2002. An extensive intercomparison between the two instruments was carried out at the time of replacement (see also section: Data visualization and availability).

TA samples were analyzed using the spectrophotometric procedure developed by Breland and Byrne (1993) and Yao and Byrne (1998). The analytical precision of the method was ± 4 µmol kg^{-1}. Certified Reference Materials (CRM) supplied by Dr. A.G. Dickson (Scripps Institution of Oceanography, USA) were measured for TA with each batch of samples. The standard deviation between the mean value of measurements of the CRM standards and the certified value was 2 µmol kg^{-1}. Details of the analysis and effects of preservation can be found in Astor *et al.* (2005) and Astor *et al.* (2013).

Estimations of total dissolved inorganic carbon, partial pressure of CO_2, and saturation state of aragonite

Total dissolved inorganic carbon (TCO_2), the partial pressure of CO_2 (pCO_2), and the saturation state for aragonite (Ω_{arag}) were estimated from the measured values of pH and TA using the program CO2SYS (Lewis and Wallace 1998). The dissociation constants used were those from of Mehrbach *et al.* (1973) as refit by Dickson and Millero (1987) for the carbonic acid (i.e., pK_1 and pK_2), Dickson (1990) for the ion HSO_4^-, and

Dickson and Riley (1979) for the HF. Precision of TCO_2 and pCO_2 estimates were derived using 1000 Monte Carlo simulations, using the average and standard deviations of pH and TA measurements. Uncertainty associated with TCO_2 was 2 µmol kg^{-1}, and for pCO_2 was 4 µatm. TCO_2 and TA were normalized to a constant salinity ($nTCO_2$ and nTA). An average salinity value for the Cariaco Basin was used, specifically S = 36.8, to remove salinity effects due to local precipitation, evaporation, and mixing (e.g., $nTCO_2 = 36.8 * TCO_2/S$).

Air-sea CO_2 flux estimations

The impurities in the pH indicator caused errors in the earlier estimates of pCO_2 of 12 ± 5 µatm in surface waters and 19 ± 8 µatm in deep waters compared to the corrected estimates. Therefore, new air-sea CO_2 fluxes were estimated for surface waters based on updated air-sea ΔpCO_2 estimates obtained from corrected pH and TA measurements, and satellite wind velocities. Air-sea CO_2 flux (F) was calculated using each set of monthly observations as follows:

$$F = k\,\alpha\,\Delta pCO_2$$

where k is the transfer velocity for air-sea CO_2 exchange, α is the solubility of CO_2 in seawater, and ΔpCO_2 is the difference between partial pressure of CO_2 in seawater (pCO_{2sea}) and the partial pressure of CO_2 in the atmosphere (pCO_{2atm}). Solubility of CO_2 was calculated according to Weiss (1974). The CO_2 gas transfer velocity was calculated using the Wanninkhof (1992) equation:

$$k = 0.31 C\,u^2\,(Sc/660)^{-0.5}$$

where u is the monthly average wind speed (units: m s^{-1}) recorded at 10 m height, Sc is the Schmidt number, and C is the nonlinearity coefficient for the quadratic term of the gas transfer relationship adjusted by Wanninkhof *et al.* (2002):

$$C = \left(\frac{1}{n}\sum_{j=1}^{n} u_j^2\right) \Big/ u_{mean}^2$$

C was calculated monthly as the ratio of the average of the daily wind squared (u_j^2) divided by the square of the average wind (u^2_{mean}). Satellite ocean wind vectors at the CARIACO station (1996-2017) were extracted from the Cross-Calibrated Multi-Platform (CCMP) gridded surface vector winds, which were produced using satellite, moored buoy, and model wind data. The CCMP Version-2.0 analyses are produced by Remote Sensing Systems and NASA. The CCMP products include four daily gridded maps at 0.25-degree resolution. Daily vector winds at the CARIACO station were calculated by averaging 4 daily wind vectors. Data for atmospheric CO_2 were taken from Dlugokencky *et al.* (2018) for Ragged Point, Barbados (13°10′N, 59°26′W) for 1996–2017. An annual average value of atmospheric CO_2 at this site was used for the calculations.

Data visualization and availability

Contour plots were generated using "Surfer® 8 from Golden Software, LLC". The T-S diagram was generated using Ocean Data View software (Schlitzer, 2018). The CARIACO data are archived and available from several locations including

the National Centers for Environmental Information (NCEI), the Ocean Carbon Data System, the Biological and Chemical Oceanography Data Management Office (BCO-DMO; CARIACO time series data: http://www.bco-dmo.org/project/2047), and the University of South Florida (http://imars.usf.edu/cariaco).

Trend analyses

For evaluating the trends for each carbonate system parameter in the water column, average monthly values were determined for three water layers. The three physical layers were identified by its potential density (explained in section Hydrography), and the monthly mean of each carbonate system parameter was calculated in the depth range that was occupied by the potential density that characterized each layer. Since the change of the Ocean Optics spectrometer model in March 2002 may have caused analytical biases that could have affected carbonate system data consistency, we calculated separately trends for the period March 2002 to January 2017, when the same instrument, indicator batch, and analytical protocol were used, and for the entire time series from December 1995 to January 2017 (Table 1).

For trend determination, the seasonal cycle was statistically removed (data were deseasonalized), by subtracting monthly observations from monthly climatologies for the two periods examined (i.e., 15-yr and 21-yr) and by adding the overall mean (*e.g.*, Bates, 2007). The deseasonalized monthly values were analyzed using a linear regression against time (decimal year) to obtain the rate of change. For pCO_2, values at the surface layer (1-7 m) were averaged to mitigate for daytime warming effects, since samples were collected close to local noon (16:30 UTC). The rate of change of deseasonalized pCO_2 was then calculated using the corrected data.

Results and Discussion

Hydrography

CARIACO time series station hydrological data (1995-2017) showed strong seasonality and interannual variability of the hydrological structure in the Cariaco Basin. Details of this variability as well as the biogeochemistry characteristics in the basin have been documented previously (Muller-Karger *et al.* 2001, Astor *et al.* 2003, Muller-Karger *et al.* 2004, Thunell *et al.* 2004, Scranton *et al.* 2006, Taylor *et al.* 2012, Scranton *et al.* 2014, Muller-Karger *et al.* 2019). Periods of strong and weak upwelling were characterized using sea surface temperature (SST), the vertical migration of the 21 ºC isotherm, and the position of the σ_θ =25 kg m^{-3} isopycnal surface (Figure 1a and 1b). Seasonal upwelling along the coast is driven by the Trade Winds and follows the seasonal migration of the Inter-Tropical Convergence Zone (ITCZ) (Muller-Karger and Aparicio 1989). The upwelling season has two periods: a period of strong upwelling between November and May and a mid-year, short-lived upwelling (~5 weeks) between July and August (Rueda-Roa 2012, Rueda-Roa *et al.* 2018). During the upwelling period, SST ranged ~23–25 ºC , increasing to 28–32 ºC during the period of stronger stratification. The strongest stratification was observed during September and October.

Table 1: Long-term trends summary statistics for different variables in the three-layer-depth system delimited by potential density (σ_θ) at the CARIACO time-series station. Surface layer (SL), Subtropical Underwater (SUW) and deep waters (DW) are represented by $\sigma_\theta < 25$, σ_θ 25-26, $\sigma_\theta > 26.4$, respectively. The trends were calculated for data beginning in March 2002 up to January 2017. During this period all measurements were done using the same equipment, same indicator batch, and same analytical protocol. The data in parenthesis correspond to the whole data set (December 1995 to January 2017) and it is reported as a matter of comparison.

Parameter	Slope	Intercept	Standard error	n	R^2	*p*-value
$\sigma_\theta < 25$						
pH	-0.003 (-0.002)	13.61 (11.49)	0.0004 (0.0002)	121 (169)	0.32 (0.28)	< 0.001
TA	0.09 (-0.14)	2238 (2689)	0.41 (0.23)	114 (160)	0.0004 (0.002)	0.83 (0.54)
nTA	0.31 (0.12)	1789 (2182)	0.41 (0.22)	114 (159)	0.005 (0.002)	0.45 (0.60)
TCO_2	2.04 (1.05)	-2023 (-30.86)	0.45 (0.26)	114 (160)	0.15 (0.10)	< 0.001
$nTCO_2$	2.23 (1.22)	-2408 (-376)	0.43 (0.24)	114 (160)	0.19 (0.14)	< 0.001
pCO_2	3.35 (2.18)	-6319 (-3975)	0.39 (0.22)	115 (161)	0.39 (0.37)	< 0.001
HCO_3^-	0.06 (0.08)	1907 (1864)	0.01 (0.02)	115 (161)	0.16 (0.13)	< 0.001
CO_3^{2-}	-1.25 (-0.73)	2755 (1704)	0.17 (0.10)	115 (161)	0.32 (0.26)	< 0.001
Ω_{arag}	-0.02 (-0.01)	42.74 (26.07)	0.003 (0.002)	115 (161)	0.31 (0.24)	< 0.001
Revelle factor	0.03 (0.02)	-48.03 (-23.31)	0.004 (0.002)	115 (161)	0.34 (0.27)	< 0.001
$\sigma_\theta = 25 - 26$						
pH	-0.003 (-0.002)	14.21 (12.03)	0.0005 (0.0003)	144 (206)	0.19 (0.19)	< 0.001
TA	0.06 (0.08)	2290 (2249)	0.30 (0.16)	135 (195)	0.0003 (0.001)	0.83 (0.62)
nTA	0.20 (0.17)	2020 (2067)	0.29 (0.16)	135 (194)	0.003 (0.006)	0.50 (0.28)
TCO_2	1.72 (1.12)	-1325 (-107)	0.40 (0.22)	136 (195)	0.12 (0.12)	< 0.001
$nTCO_2$	1.82 (1.24)	-1532 (-350)	0.42 (0.23)	136 (196)	0.12 (0.13)	< 0.001
pCO_2	3.87 (2.45)	-7325 (-4466)	0.59 (0.32)	137 (197)	0.25 (0.23)	< 0.001
HCO_3^-	2.96 (1.88)	-4038 (-1849)	0.59 (0.15)	137 (197)	0.16 (0.15)	< 0.001
CO_3^{2-}	-1.23 (-0.72)	2674 (1649)	0.24 (0.14)	137 (197)	0.16 (0.13)	< 0.001
Ω_{arag}	-0.02 (-0.01)	35.39 (23.45)	0.004 (0.002)	137 (197)	0.13 (0.12)	< 0.001
Revelle factor	0.03 (0.02)	-51.75 (-29.99)	0.007 (0.004)	137 (197)	0.14 (0.14)	< 0.001
$\sigma_\theta > 26.4$						
pH	-0.004 (-0.002)	14.91 (10.95)	0.0002 (0.0001)	138 (199)	0.77 (0.42)	< 0.001
TA	2.90 (1.89)	-3372 (-1327)	0.27 (0.18)	136 (196)	0.47 (0.37)	< 0.001
nTA	3.08 (1.89)	-3695 (-1293)	0.28 (0.18)	136 (195)	0.48 (0.36)	< 0.001
TCO_2	4.27 (2.49)	-6237 (-2657)	0.31 (0.21)	136 (196)	0.77 (0.64)	< 0.001
$nTCO_2$	4.46 (2.49)	-6586 (2613)	0.32 (0.22)	136 (195)	0.59 (0.40)	< 0.001
pCO_2	11.01 (5.59)	-21140 (-10231)	0.52 (0.42)	137 (196)	0.77 (0.48)	< 0.001
HCO_3^-	4.68 (2.73)	-7184 (-3266)	0.35 (0.24)	137 (196)	0.57 (0.40)	< 0.001
CO_3^{2-}	-0.76 (-0.36)	1622 (827)	0.04 (0.04)	137 (196)	0.76 (0.28)	< 0.001
Ω_{arag}	-0.01 (-0.01)	24.37 (12.70)	0.0006 (0.0007)	137 (196)	0.73 (0.28)	< 0.001
Revelle factor	0.06 (0.03)	-102.10 (-42.74)	0.003 (0.003)	137 (196)	0.75 (0.41)	< 0.001

The vertical distribution of water masses in the Cariaco Basin was characterized using a T-S diagram (e.g. Figure 2). The water column in the Cariaco Basin has three distinct physical potential density layers. The range depths of these layers are shown in Figure 3. Potential density differences showed a surface layer with seasonally variable temperature, a sub-surface water of Atlantic origin marked by a salinity maximum, and deep waters with colder, less saline properties. Waters with density < 25 kg m^{-3} represented the surface layer (SL) and its presence and thickness varied depending on the seasonality. It was generally located between the surface and 100 m. These surface waters can be altered by factors such as atmospheric forcing, upwelling, evaporation, precipitation, river run-off, and air-sea gas exchange. The SL had an average potential temperature of 25.85 ± 0.89 ºC, and mean salinities of 36.71 ± 0.20. A cooler and more saline layer (T = 22.37 ± 0.58 ºC and S = 36.86 ± 0.07) represented the Subtropical Underwater (SUW, Worthington 1976; Aguirre-Gómez *et al.* 2015; Qu *et al.* 2016), centered about an average depth of 100 m. SUW is characterized by having a salinity maximum of > 36.8 and a density range of 25-26 kg m^{-3} (Qu *et al.* 2016). This water mass is formed in the central subtropical gyre of the North Atlantic (Montes *et al.* 2016; Qu *et al.* 2016). During upwelling, SUW migrated vertically to shallower depths, reaching the surface during strong upwelling events. Therefore, the minimum depths of the SUW were observed between the surface and 105 m, and maximums between 30-165 m. Depth ranges oscillated between 30 and 129 m. This layer is separated from deeper waters by a transition zone (densities between 26.1–26.3 kg m^{-3}) where oxic and anoxic conditions fluctuated greatly over time due to Caribbean water intrusions into the basin (Astor *et al.* 2003, Scranton *et al.* 2014). In this transition zone, the oxygen fluctuations caused significant changes in the biogeochemical processes occurring at this level. The third layer was the deep water (DW, with depths between 175-380 m to the bottom), with nearly homogeneous densities between 26.4-26.5 kg m^{-3}. This layer had a mean temperature of 17.33 ± 0.07 ºC and mean salinity of 36.31 ± 0.02.

pH_T.

The vertical distribution of pH_T at 25 ºC at the CARIACO time series station is shown in Figure 1b (color scale). The values of pH in the surface layer ranged from 7.96 to 8.15, and its variability was controlled by seasonal upwelling and stratification. The concentration of CO_2 in the surface layer increased due to the upwelling of colder sub-surface water with lower pH and higher nutrient concentrations. Although the supply of nutrients enhanced photosynthetic activity, removing CO_2 and increasing pH, waters in this layer showed usually low pH during the upwelling period. Therefore, the interplay between the supply of CO_2 brought to the surface by upwelling and the CO_2 removal by biological activity determined the pH at the surface layer. The isopleth of pH~7.9 showed marked interannual changes in depth. This typically marked the SUW core, which was around 100 m during the stratification period (Astor *et al.* 2017) and closer or at the surface during upwelling. The values of pH decreased from 7.9 to 7.7 between 100 and 200 m. This decrease is due to remineralization of organic matter which released CO_2 due to microbial respiration. Below 300 m, pH continued slowly decreasing steadily with depth (mean 7.62 ± 0.02, ranged from 7.56 to 7.70).

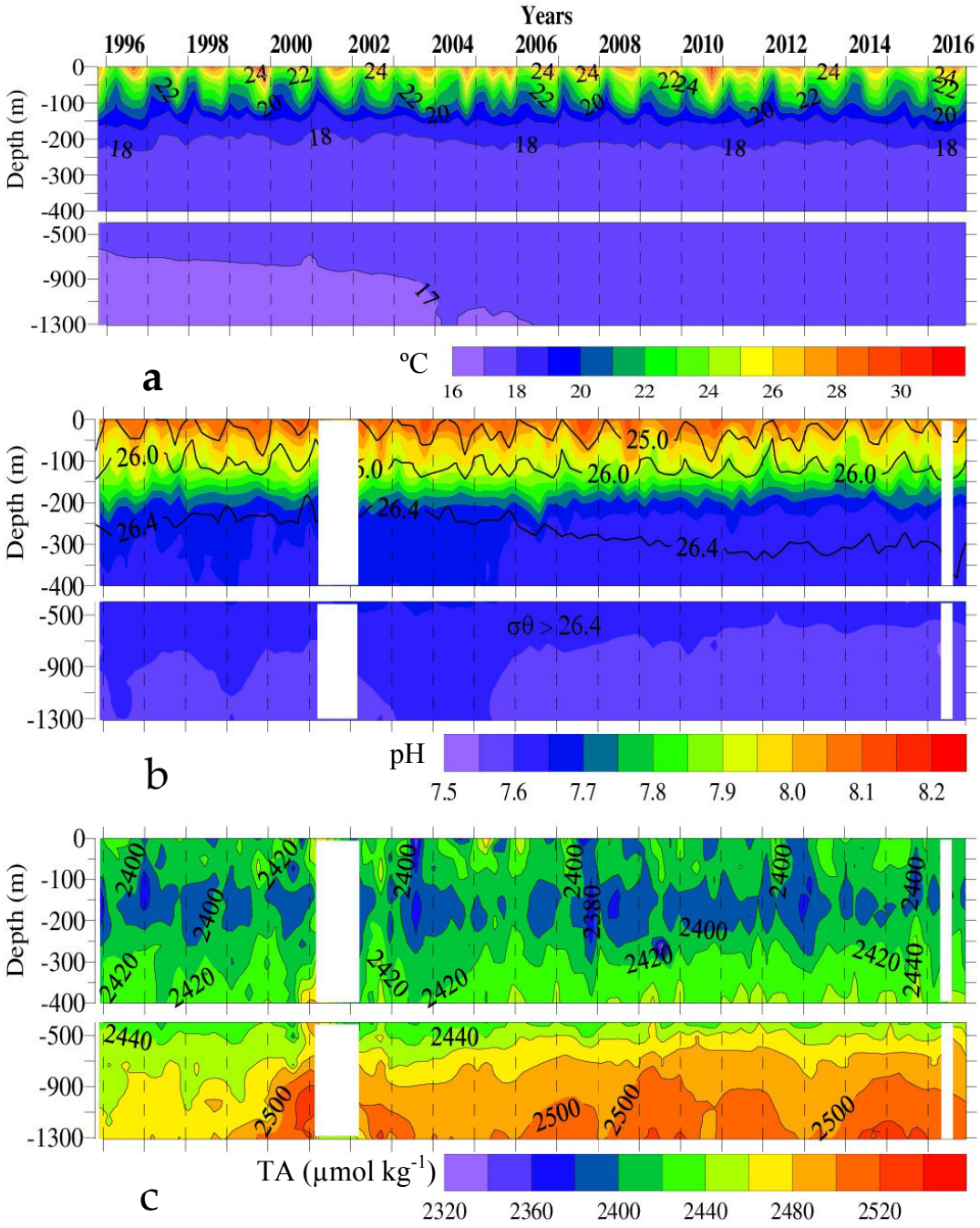

Figure 1 a-c: Seasonal and interannual variability at the CARIACO station (January 1996 to January 2017) in: (**a**) potential temperature (ºC); (**b**) pH (color scale) and σθ (isolines); (**c**) TA (µmol kg^{-1}). Blank areas indicate periods without data. Continues in the next page.

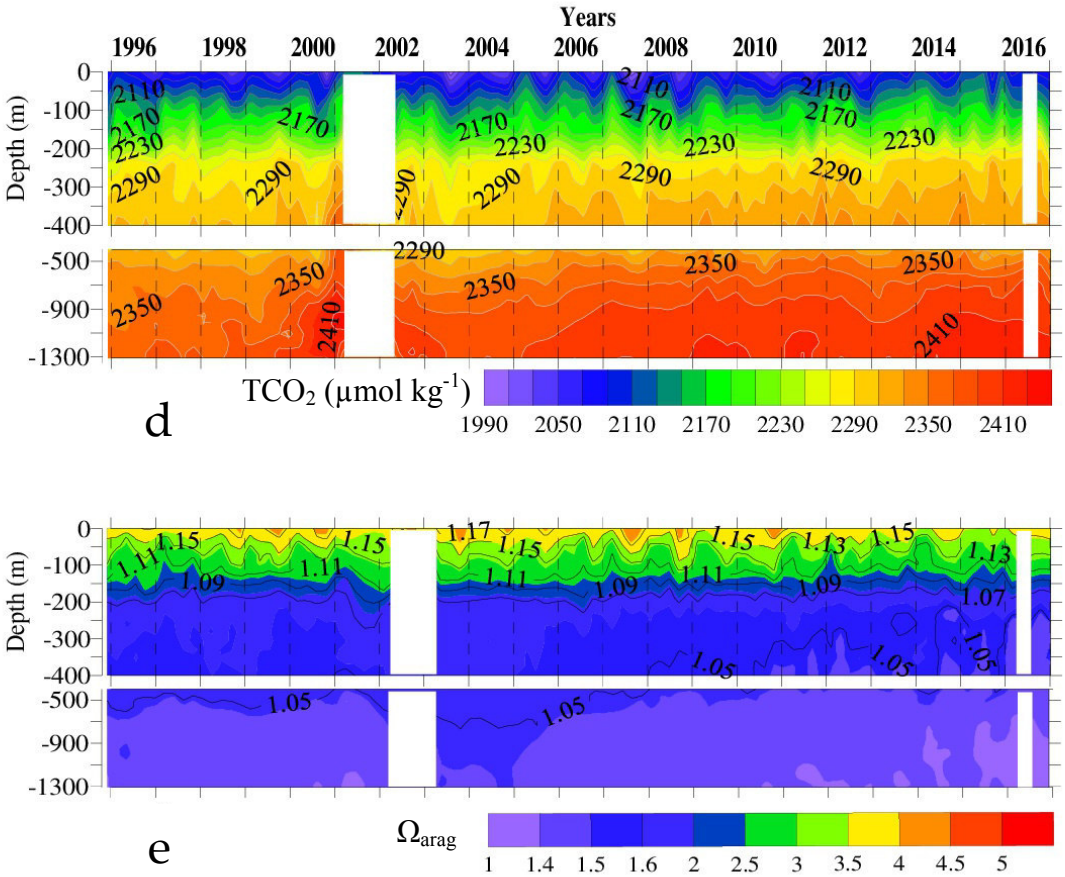

Figure 1 d-e. Seasonal and interannual variability at the CARIACO station (January 1996 to January 2017). (**d**) TCO_2 (µmol kg^{-1}), and (**e**) Omega aragonite (Ω_{arag}, color scale) and TA:TCO_2 ratio (isolines). Blank areas indicate periods without data.

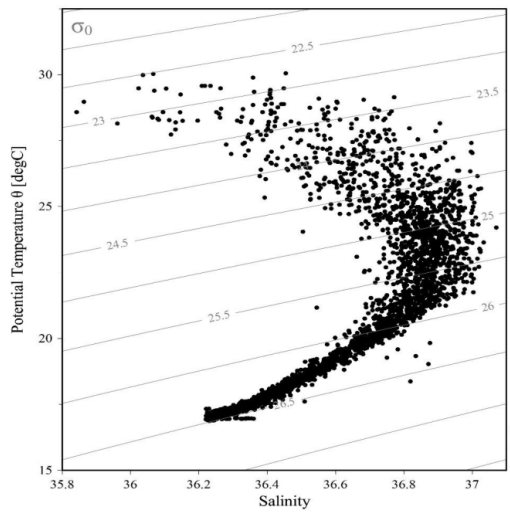

Figure 2. Potential temperature and salinity plot for the CARIACO data (January 1996 to January 2017) at all depths.

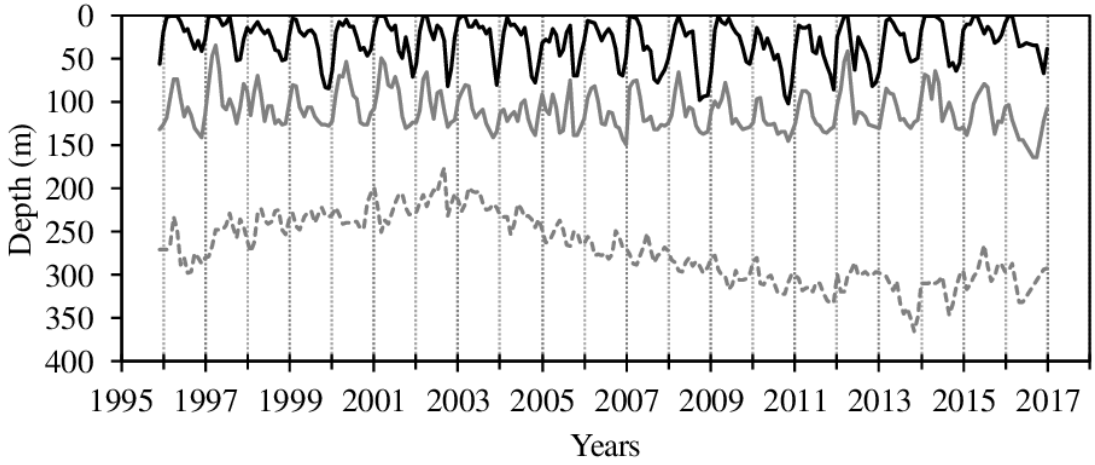

Figure 3. Seasonal and long-term variability of maximum depth of the surface layer (SL, black solid line), maximum depth of the Subtropical Underwater layer (SUW, grey solid line), and minimum depth of the deep waters layer (DW, grey dash line). The plotted lines were smoothed using a 2-month running mean.

Total alkalinity (TA)

TA showed minimal vertical structure in the upper water column (Figure 1c), with typical values between 2413 ± 19 and 2415 ± 15 μmol kg^{-1} between the SL and the SUW, respectively. Minimum values (~2394 ± 14 μmol kg^{-1}) were centered around 160 m, which is also the depth of maximum nitrification and maximum nitrate concentration (Scranton *et al.* 2014, Muller-Karger *et al.* 2019). Nitrification lowers alkalinity according to the equation:

$$NH_4^+ + 2O_2 + 2HCO_3^- \longrightarrow NO_3^- + 2H_2CO_3 + H_2O$$

Astor *et al.* (2013) reported that vertical structure in salinity had minimal effects on the TA and TCO_2 levels. Normalized TA (nTA, data not shown) showed the same vertical distribution, with average values of 2415 ± 18 and 2412 ± 14 μmol kg^{-1} between the SL and the SUW, confirming that changes in salinity due to evaporation, precipitation, mixing, and saline contribution of the SUW had only minor effect on TA. Below 200 m, TA increased steadily with depth. DW in CARIACO showed average TA values around 2458 ± 19 μmol kg^{-1}

Total inorganic carbon (TCO_2)

Figure 1d shows the vertical distribution in TCO_2 through time. Values increased with depth, with average values within the SL of 2073 ± 22 μmol kg^{-1} (range = 1983-2164 μmol kg^{-1}). Within SUW, average TCO_2 was 2131 ± 20 μmol kg^{-1} (range = 2067-2196 μmol kg^{-1}). Below that layer, average TCO_2 concentrations in the DW were 2342 ± 24 μmol kg^{-1} (range = 2266-2417 μmol kg^{-1}).

TCO_2 showed a non-conservative behavior, with high seasonal variability in the SL. In this layer, the TCO_2 concentration increase was related to the upwelling of subsurface waters rich in CO_2 during the first part of the year (January to April), while TCO_2 levels decreased slightly due to the influence of river run-off during September and October. In a few occasions, a drawdown of CO_2 was associated to events of enhanced primary production during upwelling (e.g. Astor *et al.* 2017). The vertical distribution of TCO_2 showed a steep gradient (55-60 μmol kg^{-1}) between the surface and the depth of the oxic-anoxic interface (200-300 m). This gradient was stronger during September and October 2000, 2003, 2007 and 2010. The increase of CO_2 with depth is related to rapid aerobic organic matter remineralization. This process produces CO_2, consumes O_2, but does not affect TA. Below 300 m, where anoxic waters were present, TA (in addition to TCO_2) changed due to bacterial activity such as bacterial sulfate reduction, and bacterial ammonia production (Goyet *et al.* 1991), which increased TA and TCO_2 with depth by up to 3 and 13%, respectively. Nevertheless, this relative increase in TA and TCO_2 with depth is lower than the one reported for the Black Sea (40% for both parameters), but similar to the increase with depth in the open ocean (4% for TA and 8% for TCO_2, Goyet *et al.* 1991). The ratio between TA and TCO_2 (TA:TCO_2) is used as an indicator of the relative abundance of carbonate species in seawater, and CO_2 system parameters are closely correlated to this ratio (Wang *et al.* 2013). At the CARIACO site, the TA:TCO_2 ratio decreased with depth (Figure 1e, contour lines). Below 300 m, the lowest ratios (1.03-1.06) were found, probably due to the enclosed nature of the Cariaco basin that could have favored the accumulation of remineralization products.

Saturation states of calcite and aragonite

The dissolution of CO_2 in seawater leads to an increase in the bicarbonate (HCO_3^-) and a decrease in the carbonate (CO_3^{2-}) ion concentration, pH and carbonate saturation states (Zeebe and Wolf-Gradow 2001). The water column at the CARIACO station at all depths was always supersaturated with respect to aragonite ($\Omega_{arag} > 1$) during the whole time series. Values of Ω_{arag} decreased vertically from an average SL value of 3.8 ± 0.1 to 3.2 ± 0.2 within the SUW. Below 200 m, a homogenous layer was present until the bottom, with Ω_{arag} average values of 1.5 ± 0.1. Figure 1e shows the Ω_{arag} variation with depth (color scale) and illustrates the close relationship with the TA:TCO_2 ratio found (Figure 1e, contour lines). Although the decrease in temperature with depth tends to slightly lower Ω_{arag}, the close relationship found suggests that changes in Ω_{arag} were driven more by variations in concentration of aragonite rather than those in temperature.

Temporal trends in carbonate system parameters

Table 1 shows the linear regression coefficients and standard deviation for the carbonate system parameters averaged within the three selected isopycnal intervals at the CARIACO station between March 2002 and January 2017, and December 1996 to January 2017 (in parenthesis). Anomalies of the deseasonalized time series of $nTCO_2$, nTA, pH, and Ω_{arag} for the three layers (SL, SUW, and DW) are shown in Figure 4. A significant positive trend of 2.23 ± 0.43 μmol kg^{-1} yr^{-1} ($R^2 = 0.19$, $p < 0.001$) for $nTCO_2$ was observed in the SL between March 2002 and January 2017 (Figure 4a,

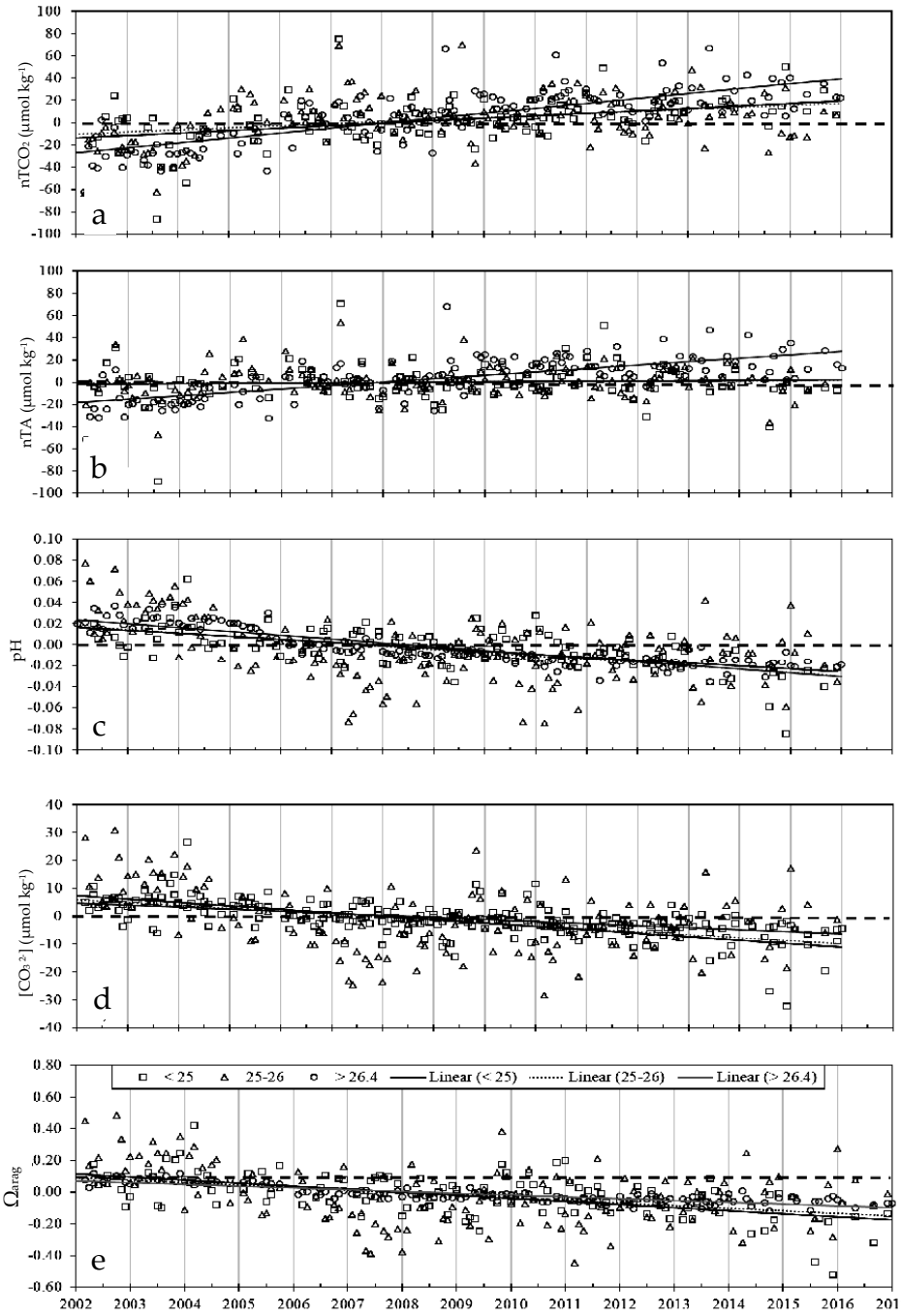

Figure 4: Time-series of the anomaly of monthly deseasonalized data of: **(a)** total $nTCO_2$ (µmol kg^{-1}), **(b)** nTA (µmol kg^{-1}), **(c)** pH, **(d)** CO_3^{-2} concentration (µmol kg^{-1}), and **(e)** Ω_{arag} at the CARIACO time-series station from March 2002 to January 2017. Squares, triangle and circles indicate data from surface (SL, $\sigma\theta < 25$), Subtropical Underwater (SUW, $\sigma\theta = 25\text{-}26$), and deep waters (DW, $\sigma\theta > 26.4$) layers, respectively. The linear trend for surface, Subtropical Underwater, and deep waters layers are indicated for a solid black straight line, a thin dot line, and a thin gray line respectively. Trends are given in Table 1.

Table 1). For comparison, $nTCO_2$ trends of 1.12 ± 0.04 µmol kg^{-1} yr^{-1} (R^2 = 0.64, $p < 0.01$) were reported for the subtropical North Atlantic at the Bermuda Atlantic Time Series (BATS) between 1983-2012, and 1.08 ± 0.08 µmol kg^{-1} yr^{-1} (R^2 = 0.55, $p < 0.01$) for the European Station Time series in the Ocean at the Canary Islands (ESTOC) between 1995-2012 (Bates *et al.* 2014). The higher rate observed in CARIACO at the surface is due to the influence of upwelling of CO_2-rich sub-surface waters (Astor *et al.* 2013). The rates of $nTCO_2$ within SUW and in the DW layer also showed an increase with values of 1.82 ± 0.42 (R^2 = 0.12, $p < 0.001$) and 4.46 ± 0.40 µmol kg^{-1} yr^{-1} (R^2 = 0.59, $p < 0.001$), respectively. The annual increase observed in the DW at the CARIACO station is over 10 times larger than the one observed at ESTOC between 300-1000 m (0.40-0.53 µmol kg^{-1} yr^{-1}, González-Davila *et al.* 2010).

Almost 95% of the particulate organic carbon (POC) produced by phytoplankton near the surface in CARIACO is consumed or regenerated within the upper 225 m of the water column (Muller-Karger *et al.* 2010). The isolated nature of the basin below sill depth (~150 m), together with the sulfate reduction of the organic carbon, allows the accumulation of CO_2 in the deep waters of the basin over time as the organic material settles through the water column. Only an average POC flux of 0.03 ± 0.03 g C m^{-2} d^{-1}, less than 2% of primary production of the surface layer, reaches the sediment on the bottom of the basin (Thunell *et al.* 2000, Muller-Karger *et al.* 2019).

TA and nTA did not show statistically significant trends within the SL and SUW. However, a significant trend was observed within the DW, with similar rates of change for TA and nTA (2.90 ± 0.27 and 3.08 ± 0.28 µmol kg^{-1}, R^2 = 0.47 and 0.48, $p < 0.001$, Figure 4b). Deep water TA and nTA showed a similar increase of 41µmol kg^{-1} from December 1995 to January 2017. This increase in TA is likely due to the dissolution of autochthonous (marine plankton) carbonates settling through the water column. Sediment traps located at the CARIACO station showed a significant decrease in the $CaCO_3$ collected in the deep sediment trap (1225 m) with respect to a shallower trap (275 m) (Goñi *et al.* 2003).

Negative slopes of pH *vs* time were found for the SL (-0.0028 ± 0.0004 yr^{-1}, R^2 = 0.32, $p < 0.001$), SUW (-0.0031 ± 0.0005 yr^{-1}, R^2 = 0.19, $p < 0.001$), and DW (-0.0036 ± 0.0002 yr^{-1}, R^2 = 0.77, $p < 0.001$). In general, the acidification rates (Figure 4c) were similar for all depths, with a tighter distribution and higher correlation in deep waters. The long-term acidification trend in the SL at CARIACO was consistent with the one reported by Bates *et al.* (2014) for the same location (-0.0025 ± 0.0004, R^2 = 0.20 and $p < 0.01$), and higher than those reported for other time series in the subtropical North Atlantic surface waters (1983-2012) such as ESTOC (−0.0018 ± 0.0002 yr^{-1}, R^2 = 0.30 and $p < 0.01$), and BATS (−0.0017 ± 0.0001 yr^{-1}, R^2 = 0.35 and $p < 0.01$) (Bates *et al.* 2014).

The increase in CO_2 levels also affects bicarbonate (HCO_3^-) and carbonate (CO_3^{2-}) ion concentrations. HCO_3^- concentration significantly increased with time (Table 1) while CO_3^{2-} concentration decreased at all depths over the period of study (Figure 4d, Table 1). The $CaCO_3$ saturation states (Ω_{arag}) also decreased with time (Figure 4e, Table 1). Ω_{arag} in the SL decreased from an initial average value of 3.92 ± 0.13 in 1996 to 3.59 ± 0.10 in 2017. Ω_{arag} deep waters decreased from 1.52 ± 0.03 in 1996 to 1.44 ± 0.02 in 2017. The 1.5 Ω_{arag} isoline shoaled from ~400 m to ~250 m over this period (Figure 1e). If this rate of decline continues with time, values of $\Omega_{arag} < 1$ may be present below 300 m by 2100 in the Cariaco Basin.

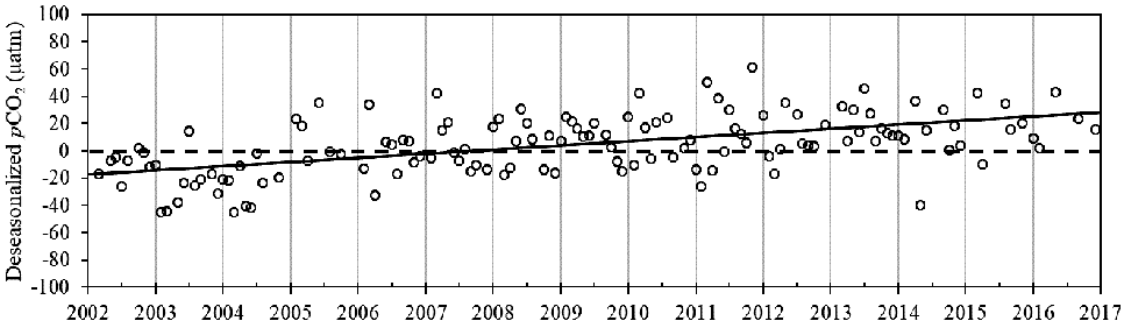

Figure 5. Time-series of the anomaly of monthly deseasonalized pCO_2 (µatm) measured in upper waters (1-7 m) at the CARIACO time-series station (March 2002 to January 2017). The linear trend is indicated for a solid black line. Trend is shown in Table 1.

Partial pressure of CO_2 and sea-air CO_2 flux

Tropical oceans are often characterized as having high pCO_2 in surface waters. They are typically a source of CO_2 to the atmosphere. CARIACO surface waters are usually supersaturated in CO_2 with respect to the atmosphere mainly because of high surface water temperatures combined with upwelling of subsurface waters (Astor *et al.* 2005). Corrected pCO_2 in the upper waters (average 1-7 m; data corrected using the ${}_{434}A_{imp}$ model) at CARIACO station was usually high with respect to pCO_{2atm}. The average of the pCO_2 surface value agreed with that reported in Astor *et al.* (2013; i.e., 392 ± 26 µatm). The rate of increase of deseasonalized pCO_2 for 2002-2017 (3.1 ± 0.42 µatm yr^{-1}; $R^2 = 0.29$, $p < 0.001$; Figure 5) was higher than that calculated for the period 1996-2008 (1.77 ± 0.43 µatm yr^{-1}, Astor *et al.* 2013). The annual mean atmospheric pCO_2 increased at 2.1 ± 0.05 µatm yr^{-1} ($R^2 = 0.99$, $p < 0.001$) between 2002-2017. Therefore, surface layer pCO_2 at the CARIACO station increased faster than pCO_2 in the atmosphere.

Sea surface pCO_2 was lower than atmospheric pCO_2 only on a few occasions, particularly during events of intense primary production. Cariaco Basin waters experienced warming during our period of observation due to a weakening in the intensity of the Trade Winds and associated upwelling (Astor *et al.* 2013, Taylor *et al.* 2012). A decrease in upwelling causes a decrease in phytoplankton productivity and weaker bloom intensities due to a reduced delivery of upwelled nutrients to the surface (Taylor *et al.* 2012). Both warming and lower primary productivity led to a steady rise in surface ocean pCO_2 over the observation period. Conditions that favored weak upwelling continued until 2012, after which winds started to increase. The positive pCO_2 trend was consistent with the rate of increase of TCO_2 and the decreasing trend of pH (Figure 4a and c).

Estimates of the air-sea flux of CO_2 are based on the air-sea pCO_2 difference (ΔpCO_2) and an estimated gas exchange coefficient (Signorini and McClain 2009). The average of net air-sea CO_2 flux for 1996-2017 was 0.6 ± 2.2 mol C m^{-2} yr^{-1}. This net air-sea CO_2 flux value is like values reported for other upwelling systems, such as the north of the Benguela system (0.56 mol C m^{-2} yr^{-1}, Santana-Casiano *et al.* 2009), and the Gulf of Oman (0.9 mol C m^{-2} yr^{-1}, Goyet *et al.* 1998). The corrected net air-sea

CO_2 flux was lower by more than 60% when compared to a previous value reported for the CARIACO station (2.0 ± 2.6 mol C m^{-2} yr^{-1}, Astor *et al.* 2013). The difference shows the cascade effect that pH uncertainties propagate into the calculation of pCO_2 and CO_2 flux, indicating the large errors associated with accepted spectrophotometric procedures used over the past 20-30 years that are based on impure indicator dyes.

The new ΔpCO_2 values confirm that the Cariaco Basin upwelling led to surface ocean supersaturation with respect to atmospheric CO_2. On average, there were 3:1 instance of positive to negative CO_2 flux values from 2002 to 2017 (n = 136). Negative CO_2 flux values indicated a net air to sea CO_2 flux, while positive values meant net CO_2 evasion from the sea (Figure 6). This result was maintained when using the whole data set (n = 196). We found surface waters supersaturated in CO_2 over the entire area of the Cariaco Basin, with a strong decreasing CO_2 flux gradient from the core of the upwelling plume, located near the CARIACO station, to areas farther offshore, during upwelling and during stratification periods (Astor *et al.* 2017). In summary, the Cariaco Basin was usually a weak source of CO_2 to the atmosphere all year-round, and only in very few limited occasions was this flux reversed.

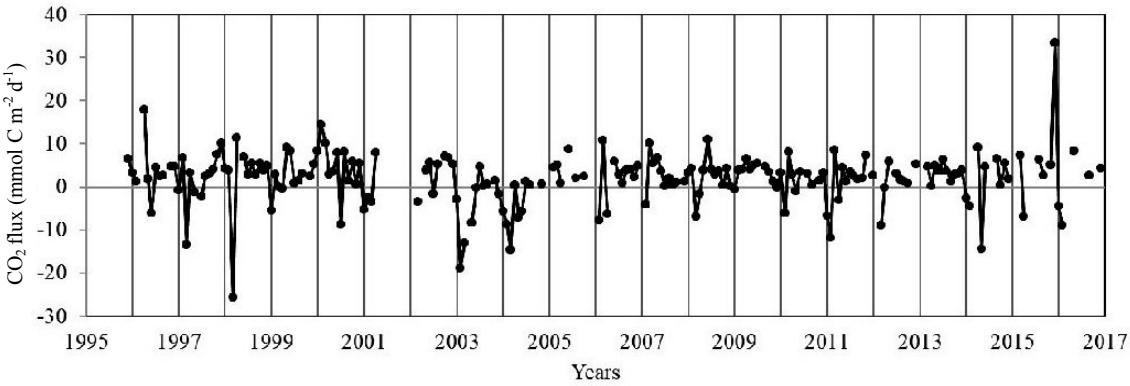

Figure 6. Time-series of CO_2 flux (mmol C m^{-2} d^{-1}) at the CARIACO time-series station from January 1996 to January 2017.

Conclusions

The CARIACO Ocean Time-Series program provided long-term monthly observations that helped to characterize seasonal and interannual variability and trends in the vertical structure of the carbonate system parameters in the Cariaco Basin. These measurements offered evidence of an increase in dissolved inorganic carbon from the surface to 1,300 m depth in a tropical coastal anoxic basin between 1995 and 2017, with the concomitant decrease in pH of these waters. For the period 2002–2017, the $nTCO_2$ increased at 2.23 ± 0.43 μmol kg^{-1} yr^{-1} within the surface mixed layer (SL). Within Subtropical Underwater (SUW), $nTCO_2$ increased by 1.82 ± 0.42 μmol kg^{-1} yr^{-1}. In waters deeper than 300 m and to the bottom (deep water or DW), $nTCO_2$ increased 4.46 ± 0.40 μmol kg^{-1} yr^{-1}.

The rise in CO_2 was linked to an increase in pCO_2 and a decrease of pH throughout the water column. The pH decreased at 0.0028 ± 0.0004 yr^{-1} for the SL, 0.0031 ± 0.0005 yr^{-1} for SUW, and 0.0036 ± 0.0002 yr^{-1} for DW. Therefore, ocean acidification was observed from the surface to the bottom, with a long-term average decrease of ~0.003 units of pH yr^{-1} for the three water layers. CO_3^{2-} ion concentration and $CaCO_3$ saturation states have also decreased with time in the Cariaco Basin. Ω_{arag} decreased 0.3 and 0.1 units for the SL and DW from December 1995 to January 2017.

Based on a correction to pH measurements that resulted from impurities in the pH indicator dye used for analyses, net air-sea CO_2 flux values presented in Astor *et al.* (2013) were revised. The recalculated pH values were used to evaluate surface ocean pCO_2 and air-sea CO_2 flux over time. The corrected surface pCO_2 values were nearly 50% lower than the uncorrected values. This highlights the importance of correcting spectrophotometric pH measurements for a bias due to indicator impurities. These pH errors cascade into biased pCO_2 estimates causing significant errors in air-sea CO_2 flux calculations. The average of the corrected net air-sea CO_2 flux for the period 1996-2017 was 0.6 ± 2.2 mol C m^{-2} yr^{-1}, indicating that the Cariaco Basin was a weak source of CO_2 to the atmosphere all year-round.

Acknowledgements

This work has been possible thanks to the collaboration of a large number of people, professionals and students, whom we cannot name all of them, but to all of them we owe the achievements obtained. In particular, we thank the staff of the "Fundación La Salle de Ciencias Naturales" of Venezuela (FLASA), the "Estación de Investigaciones Marinas de Margarita" (FLASA/EDIMAR). Countless people participated in the cruises, sample analysis and data processing such as José Jesús Narváez, Laurencia Guzmán, Jaimie Rojas, Javier Campano, Javier Gutiérrez, Patricia Ojeda, Luis González, Aitzol Arellano, Glenda Arias, Richard Bohrer, etc. We are also grateful to the crew of the B/O Hermano Ginés (FLASA). The project also benefited from the collaboration of Nahysa Martinez, Michelle L. McIntyre, Richard (Rick) Murray, Robert Thunell, Mary Scranton, Gordon Taylor, and Eric Tappa. Financially, the Project was supported by Consejo Nacional de Ciencia y Tecnología (CONICIT, VENEZUELA, 96280221), Fondo Nacional de Ciencia y Tecnología (FONACIT, Venezuela, 2000001702 and 2011000353), and LOCTI (EDIMAR 23914); National Science Foundation (NSF, USA, OCE-0752139, OCE-9216626, OCE-9729284, OCE-491 9401537, OCE-9729697, OCE-9415790, OCE-9711318, OCE -0326268, OCE-0963028, OCE-0326313, and OCE-0326268), National Aeronautics and Space Administration (NASA, USED, NAG5-6448, NAS5-97128; NNX14AP62A); and by the Inter-American Institute for Global Change Research (IAI-CRN3094).

References

AGUIRRE-GÓMEZ, R., O. SALMERÓN-GARCÍA. 2015. Characterization of the western Caribbean Sea waters through in vivo chlorophyll fluorescence. *Revista Marinas Costeras*, 7: 9-26. https://doi.org/10.15359/revmar.7.1

ASTOR Y, F. MULLER-KARGER, M. SCRANTON. 2003. Seasonal and Interannual Variation in the Hydrography of the Cariaco Basin: Implications for Basin Ventilation. *Continental Shelf Research*, 23: 125 -144. https://doi.org/10.1016/S0278-4343(02)00130-9

ASTOR, Y.M., M. I. SCRANTON, F. MULLER-KARGER, R. BOHRER, J. GARCÍA. 2005. fCO_2 variability at the CARIACO tropical upwelling time series station. *Marine Chemistry*, 97 245-261. https://doi.org/10.1016/j.marchem.2005.04.001

ASTOR, Y.M., L. LORENZONI, R. THUNELL, R. VARELA, F. MULLER-KARGER, L. TROCCOLI, G.T. TAYLOR, M.I. SCRANTON, E. TAPPA, D. RUEDA. 2013. Interannual variability in sea surface temperature and fCO_2 changes in the Cariaco Basin. *Deep Sea Research Part II: Topical Studies in Oceanography*, 93: 33-43. https://doi.org/10.1016/j.dsr2.2013.01.002

ASTOR, Y., L. LORENZONI, L. GUZMAN, G. FUENTES, F. MULLER-KARGER, R. VARELA, M. SCRANTON, G. T. TAYLOR, R. THUNELL. 2017. Distribution and variability of the dissolved inorganic carbon system in the Cariaco Basin, Venezuela. *Marine Chemistry*, 195:15-26, https://doi.org/10.1016/j.marchem.2017.08.004

BATES, N.R. 2007. Interannual variability of the oceanic CO_2 sink in the subtropical gyre of the North Atlantic Ocean over the last 2 decades, *Journal Geophysical Research*, 112, C09013, https://doi.org/10.1029/2006JC003759

BATES, N.R., M.H.P. BEST, K. NEELY, R. GARLEY, A.G. DICKSON, R.J. JOHNSON. 2012. Detecting anthropogenic carbon dioxide uptake and ocean acidification in the North Atlantic Ocean. *Biogeoscience*s, 9, 2509–2522, https://doi.org/10.5194/bg-9-2509-2012

BATES, N.R., Y.M. ASTOR, M.J. CHURCH, K. CURRIE, J.E. DORE, M. GONZÁLEZ-DÁVILA, L. LORENZONI,F. MULLER-KARGER, J. OLAFSSON, J.M. SANTANA-CASIANO. 2014. A time-series view of changing ocean chemistry due to ocean uptake of anthropogenic CO_2 and ocean acidification. *Oceanography*, 27 (1):126–141, https://doi.org/10.5670/oceanog.2014.16

BRELAND II, J.A., R.H. BYRNE. 1993. Spectrophotometric procedures for determination of seawater alkalinity using bromocresol green. *Deep-Sea Research* I, 40 (3), 629-641. https://doi.org/10.1016/0967-0637(93)90149-W

CALDEIRA, K., M.E. WICKETT. 2003. "Anthropogenic carbon and ocean pH". *Nature*, 425, 365. https://doi.org/10.1038/425365a

CLAYTON, T., R. BYRNE. 1993. Spectrophotometric seawater pH measurements: Total hydrogen ion concentration scale calibration of m-cresol purple and at-sea results, *Deep Sea Research, Part A*, 40, 2115– 2129. https://doi.org/10.1016/0967-0637(93)90048-8

DEGRANDPRE, M.D., R.S. SPAULDING, J.O. NEWTON, E.J. JAQUETH, S.E. HAMBLOCK, A.A. UMANSKY, K.E. HARRIS. 2014. Considerations for the measurement of spectrophotometric pH for ocean acidification and other studies. *Limnology Oceanography: Methods*, 12: 830-839, https://doi.org/10.4319/lom.2014.12.830

DELVALLS, T.A., A.G. DICKSON. 1998. The pH of buffers based on 2-amino-2-hydroxymethyl-1,3-propanediol ('tris') in synthetic sea water. *Deep-Sea Research. I* 45: https://doi.org/10.1016/S0967-0637(98)00019-3

DICKSON A. G. 1990. Standard potential of the reaction: $AgCl(s) + 12H_2(g) = Ag(s) + HCl(aq)$, and the standard acidity constant of the ion HSO_4^- in synthetic sea water from 273.15 to 318.15. *Journal of Chemical Thermodynamics* 22, 113-127. https://doi.org/10.1016/0021-9614(90)90074-Z

DICKSON, A.G., F.J. MILLERO. 1987. A comparison of the equilibrium constants for the dissociation of carbonic acid in seawater media. *Deep-Sea Research*. 34: 1733-1743. https://doi.org/10.1016/0198-0149(87)90021-5

DICKSON, A.G., J.P. RILEY. 1979. The estimation of acid dissociation constants in seawater media from potentiometric titrations with strong base. I. The iconic product of water-KW: *Marine Chemistry*, 7 (2), 89. https://doi.org/10.1016/0304-4203(79)90001-X

DICKSON, A. G., C.L. SABINE, J.R. CHRISTIAN (Eds.). 2007. Guide to Best Practices for Ocean CO_2 Measurements. PICES Publication 3, 191 pp. https://www.nodc.noaa.gov/ocads/oceans/Handbook_2007.html

DLUGOKENCKY, E.J., P.M. LANG, J.W. MUND, A.M. CROTWELL, M.J. CROTWELL, K.W. THONING. 2018. Atmospheric Carbon Dioxide Dry Air Mole Fractions from the NOAA ESRL Carbon Cycle Cooperative Global Air Sampling Network, 1968-2017, Version: 2018-07-31, Path: ftp://aftp.cmdl.noaa.gov/data/trace_gases/co2/flask/surface/.

DOUGLAS, N.K., R.H. BYRNE. 2017. Achieving accurate spectrophotometric pH measurements using unpurified meta-cresol purple. *Marine Chemistry*, 190: 66-72, https://doi.org/10.1016/j.marchem.2017.02.004

FRIEDLINGSTEIN, P., JONES, M. W., O'SULLIVAN, M., ANDREW, R. M., HAUCK, J., PETERS, G. P., PETERS, W., PONGRATZ, J., SITCH, S., LE QUÉRÉ, C., BAKKER, D. C. E., CANADELL, J. G., CIAIS, P., JACKSON, R. B., ANTHONI, P., BARBERO, L., BASTOS, A., BASTRIKOV, V., BECKER, M., BOPP, L., BUITENHUIS, E., CHANDRA, N., CHEVALLIER, F., CHINI, L. P., CURRIE, K. I., FEELY, R. A., GEHLEN, M., GILFILLAN, D., GKRITZALIS, T., GOLL, D. S., GRUBER, N., GUTEKUNST, S., HARRIS, I., HAVERD, V., HOUGHTON, R. A., HURTT, G., ILYINA, T., JAIN, A. K., JOETZJER, E., KAPLAN, J. O., KATO, E., KLEIN GOLDEWIJK, K., KORSBAKKEN, J. I., LANDSCHÜTZER, P., LAUVSET, S. K., LEFÈVRE, N., LENTON, A., LIENERT, S., LOMBARDOZZI, D., MARLAND, G., MCGUIRE, P. C., MELTON, J. R., METZL, N., MUNRO, D. R., NABEL, J. E. M. S., NAKAOKA, S.-I., NEILL, C., OMAR, A. M., ONO, T., PEREGON, A., PIERROT, D., POULTER, B., REHDER, G., RESPLANDY, L., ROBERTSON, E., RÖDENBECK, C., SÉFÉRIAN, R., SCHWINGER, J., SMITH, N., TANS, P. P., TIAN, H., TILBROOK, B., TUBIELLO, F. N., VAN DER WERF, G. R., WILTSHIRE, A. J., AND ZAEHLE, S. 2019. **Global Carbon Budget** 2019, *Earth Syst. Sci. Data*, 11, 1783–1838, https://doi.org/10.5194/essd-11-1783-2019

GONZÁLEZ-DÁVILA, M., J.M. SANTANA-CASIANO, M.J. RUEDA, O. LLINÁS. 2010. The water column distribution of carbonate system variables at the ESTOC site from 1995 to 2004, *Biogeosciences*, 7, 3067–3081, https://doi.org/10.5194/bg-7-3067-2010

GOÑI, M.A., R. ACEVES, R. C. THUNELL, E. TAPPA, Y. ASTOR, R. VARELA, F. MULLER-KARGER. 2003. Biogenic fluxes in the Cariaco Basin: A combined study of sinking particulates and underlying sediments. *Deep-Sea Research* I, 50: 781-807. https://doi.org/10.1016/S0967-0637(03)00060-8

GOYET, C., AL. BRADSHAW, P.G. BREWER. 1991. The carbonate system in the Black Sea. *Deep-Sea Research*, 38, Suppl. 2: 1049-1068. https://doi.org/10.1016/S0198-0149(10)80023-8

GOYET, C., R. ADAMS, G. EISCHEID. 1998. Observations of the CO_2 system properties in the tropical Atlantic Ocean. *Marine Chemistry*, 60: 49-61. https://doi.org/10.1016/S0304-4203(97)00081-9

KHATIWALA S., T. TANHUA, S. MIKALOFF FLETCHER, M. GERBER, S.C. DONEY, H.D. GRAVEN, N. GRUBER,G.A. MCKINLEY, A. MURATA, A.F. RÍOS, C.L. SABINE. 2013. Global ocean storage of anthropogenic carbon. *Biogeosciences*, 10, 2169-2191, https://doi.org/10.5194/bg-10-2169-2013

LEWIS, E., D. WALLACE. 1998. Program developed for CO_2 system calculations. Report ORNL/CDIAC -105, Carbon Dioxide Information and Analysis Center, Oak Ridge National Laboratory, U.S. Department of Energy, Oak Ridge, Tennessee, USA. https://doi.org/10.15485/1464255

LIU, X., M.C. PATSAVAS, R.H. BYRNE. 2011. Purification and characterization of meta-cresol purple for spectrophotometric seawater pH measurements. *Environmental Science Technology*, 45, 4862–4868. https://doi.org/10.1021/es200665d

MEHRBACH, C., C.H. CULBERSON, J.E. HAWLEY, R.M. PYTKOWICZ. 1973. Measurement of the apparent dissociation constants of carbonic acid in seawater at atmospheric pressure. *Limnology Oceanography*. 18: 897-907. https://doi.org/10.4319/lo.1973.18.6.0897

MONTES, E., F. MULLER-KARGER, M. W. LOMAS, A. CIANCA, L. LORENZONI, S. HABTES. 2016. Decadal variability in the oxygen inventory of North Atlantic Subtropical Underwater captured by sustained, long-term oceanographic time-series observations. *Global Biogeochemical Cycles*. https://doi.org/10.1002/2015GB005183

MULLER-KARGER F.E., R. APARICIO CASTRO. 1989. "Mesoscale processes affecting phytoplankton abundance in the southern Caribbean Sea". *Continental Shelf Research*, 14 (2-3): 199-221, https://doi.org/10.1016/0278-4343(94)90013-2

MULLER-KARGER, F.E., R. VARELA, R. THUNELL, M. SCRANTON, R. BOHRER, G. TAYLOR, J. CAPELO, Y. ASTOR, E. TAPPA, T.Y. HO, J.J. WALSH. 2001. Annual Cycle of Primary Production in the Cariaco Basin: Response to upwelling and implications for vertical export. *Journal of Geophysical Research*, 106 (C3): 4527-4542. https://doi.org/10.1029/1999JC000291

MULLER-KARGER F, R. VARELA, R. THUNELL, M. SCRANTON, G. TAYLOR, J. CAPELO, Y. ASTOR, E. TAPPA, J. AKL, T-Y. HO. 2004. Características de la Fosa de Cariaco y su importancia desde el punto de vista oceanográfico. *Memoria Fundación La Salle Ciencias Naturales La Salle*, 161-162: 215-234. Available: http://imars.marine.usf.edu/publications/caracter%C3%ADsticas-de-la-fosa-de-cariaco-y-su-importancia-desde-el-punto-de-vista

MULLER-KARGER, F.E., R. VARELA, R.C. THUNELL, M.I. SCRANTON, G.T. TAYLOR, Y. ASTOR, C.R. BENITEZ-NELSON, L. LORENZONI, K.A. FANNING, E. TAPPA, M.A. GOÑI, D. RUEDA, CH. HU. 2010. "The CARIACO oceanographic time series." *Carbon and Nutrient Fluxes in Continental Margins: a Global Synthesis, JGOFS Continental Margins Task Team (CMTT),* edited by: Liu, K.-K., Atkinson, L., Quinones, R., and Talaue-McManus, L., Springer-Verlag, Berlin Heidelberg 454. Available: http://imars.usf.edu/publications/cariaco-oceanographic-time-series

MULLER-KARGER F.E., Y.M. ASTOR, C.R. BENITEZ-NELSON, K.N. BUCK, K.A. FANNING, L. LORENZONI, E. MONTES, D.T. RUEDA-ROA, M.I. SCRANTON, E. TAPPA, G.T. TAYLOR, R.C. THUNELL, L. TROCCOLI, R. VARELA. 2019. The Scientific Legacy of the CARIACO Ocean Time-Series Program, *Annual Review of Marine Science,* 11:1, https://doi.org/10.1146/annurev-marine-010318-095150

QU, T., L. ZHANG, N. SCHNEIDER. 2016. North Atlantic Subtropical Underwater and Its Year-to-Year Variability in Annual Subduction Rate during the Argo Period. *Journal of Physical Oceanography*, 46: 1901-19016. https://doi.org/10.1175/JPO-D-15-0246.1

RUEDA-ROA, D.T. 2012. On the spatial and temporal variability of upwelling in the southern Caribbean Sea and its influence on the ecology of phytoplankton and of the Spanish sardine (*Sardinella aurita*). University of South Florida. https://scholarcommons.usf.edu/etd/4217

RUEDA-ROA, D., T. EZER, AND F. E. MULLER-KARGER. 2018. Description and mechanisms of the mid-year upwelling in the southern Caribbean Sea from remote sensing and local data. *Journal of Marine Science and Engineering*. (6):36. https://doi.org/10.3390/jmse6020036

SANTANA-CASIANO, J.M., M. GONZÁLEZ-DÁVILA, M-J. RUEDA, O. LLINÁS, E-F. GONZÁLEZ-DÁVILA. 2007. The interannual variability of oceanic CO_2 parameters in the northeast Atlantic subtropical gyre at the ESTOC site, *Global Biogeochemical Cycles*, 21, GB1015, https://doi.org/10.1029/2006GB002788

SANTANA-CASIANO, J.M., M. GONZÁLEZ-DÁVILA, I.R. UCHA. 2009. Carbon dioxide fluxes in the Benguela upwelling system during winter and spring: A comparison between 2005 and 2006. *Deep-Sea Research II*, 56: 533-541, https://doi.org/10.1016/j.dsr2.2008.12.010

SCHLITZER, R., 2018. Ocean Data View, https://odv.awi.de

SCRANTON M.I., M. MCINTYRE, G.T. TAYLOR, F. MULLER-KARGER, K. FANNING, Y. ASTOR. 2006. "Temporal Variability in the Nutrient Chemistry of the Cariaco Basin. In: Past and Present Marine Water Column Anoxia". B.B. Jørgensen, J.W. Murray and L.N. Neretin, eds. NATO Science Series: IV. Kluwer Press. Available: https://link.springer.com/content/pdf/10.1007%2F1-4020-4297-3.pdf

SCRANTON, M.I., G.T. TAYLOR, R. THUNELL, C.R. BENITEZ-NELSON, F. MULLER-KARGER, K. FANNING, L. LORENZONI, E. MONTES, R. VARELA, Y. ASTOR. 2014. Interannual and subdecadal variability in the nutrient geochemistry of the Cariaco Basin. *Oceanography*, 27 (1):148–159. https://doi.org/10.5670/oceanog.2014.18

SIGNORINI, S.R., C.R. MCCLAIN. 2009. Effect of uncertainties in climatologic wind, ocean pCO_2, and gas transfer algorithms on the estimate of global sea-air CO_2 flux. *Global Biogeochemical Cycles*, 23, GB2025, https://doi.org/10.1029/2008GB003246

TAYLOR, G.T., F.E. MULLER-KARGER, R.C. THUNELL, M.I. SCRANTON, Y. ASTOR, R. VARELA, L. TROCCOLI GHINAGLIA, L. LORENZONI, K.A. FANNING, S. HAMEED, O. DOHERTY. 2012. "Ecosystem responses in the southern Caribbean Sea to global climate change". *Proceedings of the National Academy of Sciences* Nov 2012, 109(47): 19315-19320, https://doi.org/10.1073/pnas.1207514109

THUNELL, R., R. VARELA, M. LLANO, J. COLLISTER, F. MULLER-KARGER, AND R. BOHRER. 2000. "Organic carbon flux in an anoxic water column: sediment trap results from the Cariaco Basin". *Limnology and Oceanography*. 45. 300-308. https://doi.org/10.4319/lo.2000.45.2.0300

THUNELL R.C., D.M. SIGMAN, F. MULLER-KARGER, Y. ASTOR, R. VARELA. 2004. "Nitrogen isotope dynamics of the Cariaco Basin, Venezuela". Global Biochemical Cycles, 18, GB3001, https://doi.org/10.1029/2003GB002185

WANG Z.A., R. WANNINKHOF, W.-J. CAI, R.H. BYRNE, X. HU, T.-H. PENG, W.-J. HUANG. 2013. The marine inorganic carbon system along the Gulf of Mexico and Atlantic coasts of the United States: Insights from a transregional coastal carbon study. *Limnology Ocanography*, 58 (1): 325-342. https://doi.org/10.4319/LO.2013.58.1.0325

WANNINKHOF, R., 1992. Relationship between gas exchange and wind speed over the ocean. *Journal Geophysical Research*, 97, 7373–7381, https://doi.org/10.1029/92JC00188

WANNINKHOF, R., S.C. DONEY, T. TAKAHASHI, W.R. MCGILLIS. 2002. The effect of using time-averaged winds on regional air-sea CO_2 fluxes, in Gas Transfer at Water Surfaces, Geophysical Monograph Series, vol. 127, edited by M.A. Donelan et al., pp. 351–356, AGU, Washington, D.C. https://doi.org/10.1029/GM127P0351

WEISS, R.F. 1974. Carbon dioxide in water and seawater: The solubility of a non-ideal gas. *Marine Chemistry*. 2: 203-215. https://doi.org/10.1016/0304-4203(74)90015-2

WORTHINGTON, L.V. 1976. On the North Atlantic Circulation. Johns Hopkins University Press, 110.

YAO, W., R.H. BYRNE. 1998. Simplified seawater alkalinity analysis: use of linear array spectrometers. *Deep-Sea Research. I* 45: 1383-1392. https://doi.org/10.1016/S0967-0637(98)00018-1

YAO, W., X. LIU, R. BYRNE. 2007. Impurities in indicators used for spectrophotometric pH measurements: Assessments and remedies, *Marine Chemistry*, 107, 167–172, https://doi.org/10.1016/j.marchem.2007.06.012

ZEEBE, R.E., D. WOLF-GLADROW. 2001. CO_2 in seawater: equilibrium, kinetics, isotopes. Nº 65. Elsevier. http://geosci.uchicago.edu/~kite/doc/Zeebe_CO2_In_Seawater_Ch_1.pdf

Recibido: 4 noviembre 2022
Aceptado: 22 agosto 2023
Publicado en línea: 12 noviembre 2023

Yrene M. Astor [1], Laura Lorenzoni [2], Digna Rueda-Roa [2], Frank Muller-Karger [2]

[1] Estación de Investigaciones Marinas de Margarita, Fundación La Salle de Ciencias Naturales, Punta de Piedras, Estado Nueva Esparta, Venezuela.
Email: yrene.astor@yahoo.com

[2] College of Marine Science, University of South Florida, St. Petersburg, Florida 33701, USA.
Email: carib@usf.edu